

## 对位取代苯甲酸与 2,2'-联吡啶配体构筑的 两种二价铅配合物的合成、晶体结构及性质

杨娟\* 缪娟 戴俊 杨磊 张丽娜

(河南理工大学理学院, 焦作 454003)

**摘要:** 水热条件下, 合成了 2 个含对位取代苯甲酸和 2,2'-联吡啶配体的二价铅配合物  $[\text{Pb}(\text{4-HOBA})_2(2,2'\text{-bipy})] \cdot \text{H}_2\text{O}$  (4-HOBAH=4-hydroxybenzoic acid, 2,2'-bipy=2,2'-bipyridine) (**1**) 及  $[\text{Pb}(\text{4-MBA})_2(2,2'\text{-bipy})]$  (4-MBAH=4-methylbenzoic acid) (**2**), 并通过 X-射线单晶结构分析、元素分析、红外光谱、紫外光谱、荧光光谱以及热重分析等手段对配合物进行了表征与研究。X-射线单晶结构测定表明, 2 种晶体的不对称单元中, 六配位的二价铅离子分别与来自 1 个 2,2'-联吡啶的 2 个 N 原子和 2 个对位取代苯甲酸的 4 个 O 原子螯合。配合物 **1** 属单斜晶系,  $P2_1/c$  空间群,  $a=1.094\ 83(4)\text{ nm}$ ,  $b=1.751\ 94(6)\text{ nm}$ ,  $c=1.204\ 79(4)\text{ nm}$ ,  $\beta=100.334(2)^\circ$ ,  $V=2.273\ 39(14)\text{ nm}^3$ ,  $Z=4$ , final  $R_1=0.025\ 4$ ,  $wR_2=0.067\ 4$ 。广泛存在的分子间氢键和弱  $\pi\cdots\pi$  堆积作用将配合物 **1** 组装成稳定的三维超分子结构。配合物 **2** 属三斜晶系,  $P\bar{1}$  空间群,  $a=0.955\ 10(11)\text{ nm}$ ,  $b=1.008\ 05(12)\text{ nm}$ ,  $c=1.324\ 83(15)\text{ nm}$ ,  $\alpha=109.865(1)^\circ$ ,  $\beta=97.322(1)^\circ$ ,  $\gamma=90.643(1)^\circ$ ,  $V=1.187\ 8(2)\text{ nm}^3$ ,  $Z=2$ , final  $R_1=0.028\ 4$ ,  $wR_2=0.050\ 8$ 。配合物 **2** 经由一对  $\text{Pb}\cdots\text{O}(0.318\ 5(2)\text{ nm})$  弱相互作用被组装成二聚体结构, 弱的  $\text{Pb}\cdots\text{O}$  相互作用及与配合物 **1** 中类似的  $\pi\cdots\pi$  堆积作用共同构筑了配合物 **2** 的三维结构。在配合物 **1** 和 **2** 中, 铅的 6s 孤电子均显示了立体化学活性, 使配位键分布于半球型区域。同时, 两种配合物固体均具有光致发光特性, 并在蓝光区有较强发射。

**关键词:** 铅配合物; 4-羟基苯甲酸; 4-甲基苯甲酸; 晶体结构

中图分类号: O614.43\*3

文献标识码: A

文章编号: 1001-4861(2010)11-1992-09

## Syntheses, Crystal Structures and Properties of Two Lead (II) Complexes with Para-Substituted Benzoic Acid and 2,2'-Bipyridine Co-Ligand

YANG Juan\* MIAO Juan DAI Jun YANG Lei ZHANG Li-Na

(Department of Physical Chemistry, Henan Polytechnic University, Jiaozuo, Henan 454003)

**Abstract:** Two mononuclear Lead(II) complexes  $[\text{Pb}(\text{4-HOBA})_2(2,2'\text{-bipy})] \cdot \text{H}_2\text{O}$  (**1**) and  $[\text{Pb}(\text{4-MBA})_2(2,2'\text{-bipy})]$  (**2**) were isolated from the hydrothermal reaction of 4-hydroxybenzoic acid (4-HOBAH), 4-methylbenzoic acid (4-MBAH), 2,2'-bipyridine (2,2'-bipy) and  $\text{Pb}(\text{CH}_3\text{COO})_2 \cdot 3\text{H}_2\text{O}$ , and characterized by elemental analysis, IR, UV, TG and single-crystal X-ray structure analysis. In these two complexes, Pb(II) ions are six-coordinated and chelated by two N atoms from one 2,2'-bipy ligand and four O atoms from two para-benzonate ligands. Complex **1** crystallizes in the monoclinic system, space group  $P2_1/c$  with  $a=1.094\ 83(4)\text{ nm}$ ,  $b=1.751\ 94(6)\text{ nm}$ ,  $c=1.204\ 79(4)\text{ nm}$ ,  $\beta=100.334(2)^\circ$ ,  $V=2.273\ 39(14)\text{ nm}^3$ ,  $Z=4$ , final  $R_1=0.025\ 4$ ,  $wR_2=0.067\ 4$ . The extensive hydrogen bonds and weak  $\pi\cdots\pi$  stacking effects assemble and stabilize the 3D supramolecular structure. Complex **2** crystallizes in the triclinic system, space group  $P\bar{1}$  with  $a=0.955\ 10(11)\text{ nm}$ ,  $b=1.008\ 05(12)\text{ nm}$ ,  $c=1.324\ 83(15)\text{ nm}$ ,  $\alpha=109.865(1)^\circ$ ,  $\beta=97.322(1)^\circ$ ,  $\gamma=90.643(1)^\circ$ ,  $V=1.187\ 8(2)\text{ nm}^3$ ,  $Z=2$ , final  $R_1=0.028\ 4$ ,  $wR_2=0.050\ 8$ . The complex **2** molecules related by inversion center are organized into dimeric units via a pair of  $\text{Pb}\cdots\text{O}$  interactions of  $0.318\ 5(2)\text{ nm}$ . The weak  $\text{Pb}\cdots\text{O}$  interactions and similar  $\pi\cdots\pi$  stacks with complex **1**, construct the complex **2** into a stable three-

收稿日期: 2010-03-08。收修改稿日期: 2010-06-10。

国家自然科学基金(No.20901028)和河南理工大学博士基金(No.B2008-58648265)资助项目。

\*通讯联系人。E-mail: yangjuan0302@yahoo.cn

第一作者: 杨娟, 女, 30 岁, 博士, 副教授; 研究方向: 无机材料及功能配合物。

dimensional supramolecular structure. In both complexes **1** and **2**, the 6s lone pair of electrons of Pb<sup>II</sup> atom has a stereochemistry activity resulting the distribution of the bonds in a hemisphere. The photoluminescence properties of these two complexes in the solid state were also studied at room temperature and strong blue emissions were observed. CCDC: 765050, **1**; 767116, **2**.

**Key words:** lead complex; 4-hydroxybenzoic acid; 4-methylbenzoic acid; crystal structure

Complexes containing Pb(II) ion have recently attracted considerable research interests not only because of their intriguing variety of architectures but also because of their fascinating potential application in different fields, especially in environmental protection due to the toxicity of lead and in biological systems for its diverse interactions with biological molecules<sup>[1-3]</sup>. In general, Pb(II) complexes can adopt diverse coordination numbers from 2 to 10 and rich coordination geometry<sup>[4]</sup>, deriving from large radius like lanthanide ions and the possible occurrence of a stereochemically active lone pair of electrons<sup>[5]</sup>. For low coordination numbers (2~5), the lone pair is stereochemically active and the ligand-to-metal bonds are distributed unevenly around the metal center with an identifiable void (presumably the location of the lone pair) present in the coordination sphere, resulting in a “hemidirected” ligand environment<sup>[4]</sup>. On the other hand, complexes with high coordination numbers (9~10) adopt a holodirected geometry in which the ligands are distributed evenly throughout the coordination sphere with a stereochemically inactive lone pair. For intermediate coordination numbers (6~8), the stereochemical activity of the lone pair, and hence the geometry, depends strongly on the nature of the ligands and the donor atoms. Generally, complexes with large, bulky ligands and with soft donors have a stereochemically inactive lone pair and holodirected geometries<sup>[4]</sup>.

To the best of our knowledge, carboxylate coordinates metal in various ways<sup>[6-9]</sup>, for example, in the mode of monodentate, bidentate chelating, bidentate bridging or chelating-bridging. As rigid ligands, benzoic acid and its derivatives have been widely used to build organic-inorganic hybrid materials with the high thermal stability<sup>[10]</sup>. Furthermore, the chelating aromatic amine 2,2'-bipyridine (2,2'-bipy) as co-ligands can

effectively increase the stability of the structure and fluorescent properties, due to the  $\pi \cdots \pi$  stacking and the hydrogen-bonds formed between the carboxyl oxygen atoms and the pyridine nitrogen atoms.

Although numerous successful macrocyclic ligands for coordinating main-group metal Pb<sup>2+</sup> ( $5d^{10}6s^2$ ) have been reported in the literature<sup>[11-13]</sup>, the study of Pb(II) complexes constructed by carboxyl acids and 2,2'-bipy ligands has been lacking so far. With the aim of preparing stable functional Pb(II) complexes, we used benzoic acid with different para-substituted groups, that is, 4-hydroxybenzoic acid (4-HOBAH) and 4-methylbenzoic acid (4-MBAH) as ligands with the rigid 2,2'-bipy as co-ligand, and obtained two new complexes [Pb(4-HOBA)<sub>2</sub>(2,2'-bipy)] · H<sub>2</sub>O (**1**) and [Pb(4-MBA)<sub>2</sub>(2,2'-bipy)] (**2**) prepared by hydrothermal method. The crystal structures, thermal stabilities and luminescent properties of the complexes are reported in this paper.

## 1 Experimental

### 1.1 Reagents and instruments

Pb(CH<sub>3</sub>COO)<sub>2</sub> · 3H<sub>2</sub>O, 4-hydroxybenzoic acid, 4-methylbenzoic acid, 2,2'-bipyridine, DMSO and so on are analytically pure grade and used without further purification. Infrared spectra were collected with a FTIR Thermo Nicolet Impact 410 spectrometer with KBr pellets in the 4 000~400 cm<sup>-1</sup> regions. Elemental (C, H and N) analysis were performed on a Perkin-Elmer 2400LS analyzer. The UV-Vis spectra were measured in DMSO solvent ( $c=0.1$  mmol · L<sup>-1</sup>) by a UV-260 spectrophotometer. Thermogravimetric analyses were conducted on a Perkin Elmer TG-7 with a heating rate of 10 °C · min<sup>-1</sup> from 30 to 700 °C under N<sub>2</sub> stream. The luminescent spectra of the complexes were recorded at room temperature on a Hitachi F-4500 fluorescence spectrofluorometer (the pass width is

5.0 nm).

## 1.2 Syntheses of compounds **1** and **2**

Complex **1** was synthesized by hydrothermal method in a 25 mL Teflon-lined autoclave by heating a mixture of 5.2 mmol  $\text{Pb}(\text{CH}_3\text{COO})_2 \cdot 3\text{H}_2\text{O}$ , 8.4 mmol 4-hydroxylbenzoic acid, 2.1 mmol 2,2'-bipyridine and 10 mL distilled water at 170 °C for 7 d. Colorless block single crystals were collected by filtration and washed by water and ethanol for three times with a yield of 65% based on Pb. Anal. Calcd. for  $\text{C}_{24}\text{H}_{20}\text{N}_2\text{O}_7\text{Pb}$  (%): C, 43.97; H, 3.07; N, 4.27. Found (%): C, 43.82; H, 3.03; N, 4.21.

Complex **2** was obtained by the same synthetic procedure as that for **1** except using 4-methylbenzoic acid instead of 4-hydroxylbenzoic acid. Colorless prism crystals of **2** were collected by filtration and washed by water and ethanol for three times with a yield of 52% based on Pb. Anal. Calcd. for  $\text{C}_{26}\text{H}_{22}\text{N}_2\text{O}_4\text{Pb}$  (%): C, 49.28; H, 3.50; N, 4.42. Found (%): C, 48.05; H, 3.47;

N, 4.36.

## 1.3 X-ray crystal structure determination

The X-ray diffraction measurements for **1** and **2** were performed on Bruker SMART APEX II CCD diffractometer with graphite-monochromatized Mo  $K\alpha$  radiation ( $\lambda=0.071\ 073\ \text{nm}$ ) by using  $\varphi$ - $\omega$  scan mode at 296(2) K. Empirical absorption correction was applied to the intensity data using the SADABS program<sup>[14]</sup>. The structures were solved by direct methods and refined by full-matrix least-square on  $F^2$  using the SHELXTL-97 program<sup>[15]</sup>. All non-hydrogen atoms were refined anisotropically. All the hydrogen atoms bonded to carbon atoms and the hydroxyl hydrogen atoms were generated geometrically and refined isotropically using the riding model. The hydrogen atoms of the water molecules were located in a difference Fourier map. Details of the crystal parameters, data collection and refinements for **1** and **2** are summarized in Table 1.

CCDC: 765050, **1**; 767116, **2**.

Table 1 Crystallographic data and structure refinement of complex **1** and **2**

Complex	<b>1</b>	<b>2</b>
Empirical formula	$\text{C}_{24}\text{H}_{20}\text{N}_2\text{O}_7\text{Pb}$	$\text{C}_{26}\text{H}_{22}\text{N}_2\text{O}_4\text{Pb}$
Formula weight	655.61	633.65
Crystal system	Monoclinic	Triclinic
Space group	$P2_1/c$	$P\bar{1}$
$a / \text{nm}$	1.094 83(4)	0.955 10(11)
$b / \text{nm}$	1.751 94(6)	1.008 05(12)
$c / \text{nm}$	1.204 79(4)	1.324 83(15)
$\alpha / (^\circ)$		109.865(1)
$\beta / (^\circ)$	100.334(2)	97.322(1)
$\gamma / (^\circ)$		90.643(1)
$Z$	4	2
$V / \text{nm}^3$	2.273 39(14)	1.187 8(2)
$D / (\text{g} \cdot \text{cm}^{-3})$	1.915	1.772
$\mu / \text{mm}^{-1}$	7.47	7.14
$F(000)$	1 264	612
Crystal size / mm	0.35×0.26×0.21	0.35×0.26×0.18
$\theta$ range for data collection / $(^\circ)$	2.2 to 26.9	2.2 to 26.6
Reflections collected	18 618	14 285
Independent reflections ( $R_{\text{int}}$ )	4 067 (0.037)	5 555 (0.027)
Observed reflections ( $I > 2\sigma(I)$ )	3 579	4 965
Final GooF	1	1.02
$R_1, wR_2$ ( $I > 2\sigma(I)$ )	0.025 4, 0.067 4	0.028 4, 0.050 8
$R_1, wR_2$ (all data)	0.031 6, 0.071 6	0.022 9, 0.049 1
Largest different peak and hole / $(\text{e} \cdot \text{nm}^{-3})$	1 051, -608	774, -763

## 2 Results and discussion

### 2.1 Structure description

#### 2.1.1 Crystal structure of complex **1**

The asymmetric unit of the complex **1** is shown in Fig.1. Selected bond distances and angles are listed in Table 2. In the complex, Pb<sup>II</sup> ion is chelated by two N atoms of one 2,2'-bipy ligand, four O atoms from two 4-HOBA ligands. The coordination number is 6 with a PbN<sub>2</sub>O<sub>4</sub> chromophore. There are one five-membered ring formed by lead atom and bidentate chelating 2,2'-bipy ligand and two four-membered rings formed by lead atom and 4-HOBA ligands. The two rings of the 2,2'-bipy ligand are nearly coplanar with a dihedral angle of 2.66(19)°, which is similar to the recent reference<sup>[3]</sup>. The Pb1-N bond distances are 0.246 3(3) and 0.256 3(3) nm, which are in good agreement with the reported values<sup>[16-17]</sup>. The Pb1-O bond lengths are in the range of 0.247 7(3) to 0.262 5(3) nm. The bond angles around Pb(II) are in the range of 50.89(8)° and 154.53(9)° (Table 2). The bond angles between Pb1<sup>II</sup> ion and the coordinated atoms O1, O2, O5, O4 are 50.89(8)° (O5-Pb1-O4), 83.20(9)° (O5-Pb1-O2), 51.53(9)° (O2-Pb1-O1), and 154.53(9)° (O1-Pb1-O4), respectively. The sum of these bond angles is 340.15°, which indica-

tes that O1, O2, O5, O4 and Pb1 are incompletely coplanar. The atom N1 and N2 lie in the axial position. The bond angles between N1 and the atoms of equatorial plane are N1-Pb1-O1 81.27(11)°, N1-Pb1-O2 77.93(10)°, N1-Pb1-O5 76.79(10)° and N1-Pb1-O4 75.54(10)°, all of which deviate to 90°. The apical atom N2 has similar bond angles to N1, which demonstrates that both N1 and N2 do not lie in the center axis of the equatorial plane. Hence, the hexa-coordinated Pb<sup>II</sup> center adopts a severe distorted hemidirected coordination environment, which N1 and N2 of 2,2'-bipy lie in the apical position in complex **1**.

The stereochemical activity of the lone pair of

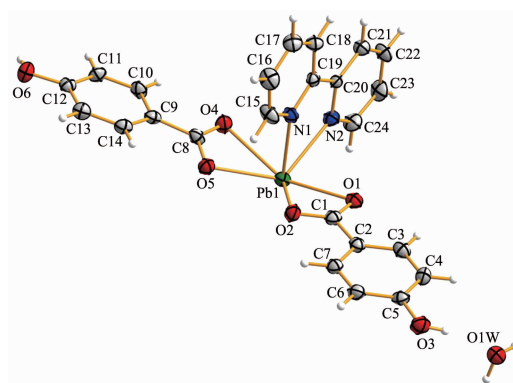


Fig.1 Asymmetric unit of complex **1** with the atom numbering

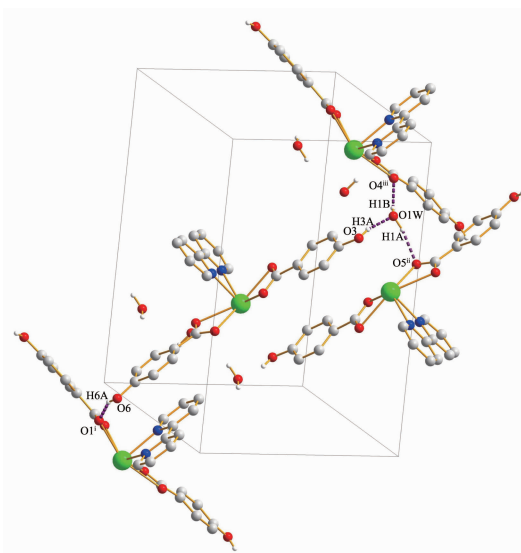
Table 2 Selected bond distances (nm) and bond angles (°) for complex **1** and **2**

1					
Pb1-N1	0.246 3(3)	Pb1-O5	0.251 4(3)	Pb1-O1	0.258 3(3)
Pb1-O2	0.247 7(3)	Pb1-N2	0.256 3(3)	Pb1-O4	0.262 5(3)
N1-Pb1-O2	77.93(10)	N1-Pb1-O5	76.79(10)	O2-Pb1-O5	83.20(9)
N1-Pb1-N2	64.57(10)	O2-Pb1-N2	123.60(11)	O5-Pb1-N2	123.38(10)
O1-Pb1-N1	81.27(11)	O1-Pb1-O2	51.53(9)	O1-Pb1-O5	132.96(8)
N2-Pb1-O1	81.23(9)	N1-Pb1-O4	75.54(10)	O2-Pb1-O4	130.87(9)
O4-Pb1-O5	50.89(8)	N2-Pb1-O4	79.42(10)	O1-Pb1-O4	154.53(9)
2					
Pb1-O1	0.233 3(2)	Pb1-O3	0.241 8(2)	Pb1-N2	0.260 8(3)
Pb1-O2	0.264 4(2)	Pb1-N1	0.265 6(3)	Pb1-O4	0.270 1(2)
O1-Pb1-O3	84.31(9)	O1-Pb1-N2	83.74(8)	O3-Pb1-N2	77.33(8)
O1-Pb1-O2	52.25(7)	O3-Pb1-O2	121.72(8)	N2-Pb1-O2	124.68(8)
O1-Pb1-N1	79.77(8)	O3-Pb1-N1	137.27(8)	N2-Pb1-N1	61.75(8)
O2-Pb1-N1	77.17(8)	O1-Pb1-O4	82.72(8)	O3-Pb1-O4	50.77(8)
N2-Pb1-O4	127.29(8)	O2-Pb1-O4	83.26(7)	N1-Pb1-O4	159.20(9)

electrons on the lead (II) is an interesting issue, which is always discussed. The fundamental geometrical features with an active lone pair are usually a vacancy of coordination in the region where the lone pair is thought to be located and a shortening of the Pb-donor bond lying in the opposite side of the lead center relative to the proposed site of the lone pair<sup>[18]</sup>. For the complex **1**, it can be seen from the data of Table 2 that there is an obvious gap in the coordination spheres of Pb<sup>II</sup> ions, for example, the bond angle (O1-Pb1-O5) is 132.96(8)°. These results demonstrate the stereochemical activity of the lone pair of electrons and the coordination sphere of Pb<sup>II</sup> ions is hemidirected in complex **1**. Among these coordinated bonds, the bond (Pb1-N1) is shortest and the bond (Pb1-O4) is longest. Therefore, the lone pair of electrons in 6s orbit around Pb<sup>II</sup> can be considered to lie in the opposite direction of Pb1-N1 and close to the bond of Pb1-O4, as shown in Fig.7.

The hydroxyl groups of 4-HOBA ligands are all nonbonding with Pb<sup>2+</sup> ions, but form the rich hydrogen bonds with the adjacent carboxyl oxygen atoms and free water molecules. Additionally, there also exist the

intermolecular hydrogen bonds between free water molecules and the adjacent carboxyl oxygen atoms, as shown in Table 3 and Fig.2. The hydrogen bond lengths and angles of O-H···O are 0.267 1(4)~0.284 9(4) nm and 148°~166°.



Symmetry codes: <sup>i</sup>  $-x, 0.5+y, 0.5-z$ ; <sup>ii</sup>  $1-x, 1-y, -z$ ; <sup>iii</sup>  $1-x, -0.5+y, 0.5-z$

Fig.2 Hydrogen-bonding interactions of complex **1**

Table 3 Hydrogen bond lengths and angles

D-H···A	D-H / nm	H···A / nm	D···A / nm	∠DHA / (°)
O6-H6A···O1 <sup>i</sup>	0.082	0.190	0.267 1(4)	156.8
O3-H3A···O1W	0.082	0.189	0.269 5(5)	166.4
O1W-H1A···O5 <sup>ii</sup>	0.090(3)	0.204(3)	0.284 9(4)	148(5)
O1W-H1B···O4 <sup>iii</sup>	0.083(3)	0.200(3)	0.278 9(4)	158(5)

Symmetry codes: <sup>i</sup>  $-x, 0.5+y, 0.5-z$ ; <sup>ii</sup>  $1-x, 1-y, -z$ ; <sup>iii</sup>  $1-x, -0.5+y, 0.5-z$ .

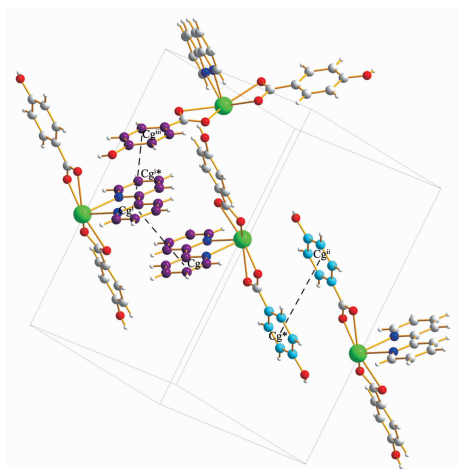
In addition to the hydrogen bonds, there are three kinds of weak inter-molecular  $\pi \cdots \pi$  stacking interactions of the parallel benzene rings of 4-HOBA ligands, pyridyl rings of 2,2'-bipy and between the benzene ring and pyridyl ring belonging to the adjacent structure units. As shown in Fig.3, the pyridyl ring (N1, C15, C16, C17, C18, C19, centroid C<sub>g</sub><sup>i</sup>) and the adjacent ring (N2, C20, C21, C22, C23, C24, centroid C<sub>g</sub><sup>ii</sup>, symmetry code: <sup>i</sup>  $2-x, 1-y, 1-z$ ) are parallel with  $d_{C-C}=0.411\ 22$  nm,  $d_{P-P}=0.337\ 89$  nm and  $\theta=2.535^\circ$ , in which C<sub>g</sub> is the ring centroid,  $d_{C-C}$  is the centroid-centroid distance,  $d_{P-P}$  is the vertical distance, and  $\theta$  is the dihedral angle of two neighboring  $\pi$ -planes. Similarly, the benzene ring (C2, C3, C4, C5, C6, C7, centroid C<sub>g</sub><sup>iii</sup>) and the

neighboring ring (centroid C<sub>g</sub><sup>ii</sup>, symmetry code: <sup>ii</sup>  $1-x, 1-y, 2-z$ ) are parallel highly with  $d_{C-C}=0.470\ 15$  nm,  $d_{P-P}=0.348\ 16$  nm and  $\theta=0.699^\circ$ . The pyridyl ring (N1, C15, C16, C17, C18, C19, centroid C<sub>g</sub><sup>i\*</sup>) and the adjacent benzene ring (C9, C10, C11, C12, C13, C14, centroid C<sub>g</sub><sup>iii</sup>, symmetry code: <sup>iii</sup>  $x, 0.5-y, -0.5+z$ ) are also parallel with  $d_{C-C}=0.384\ 83$  nm,  $d_{P-P}=0.339\ 72$  nm and  $\theta=2.750^\circ$ . The extensive hydrogen-bonding and weak  $\pi \cdots \pi$  interactions lead to self-assembled molecular conformation and contribute to the stable three dimensional supramolecular structures.

### 2.1.2 Crystal structure of complex **2**

In spite of the same synthetic methods and the similar ligands used in the complex **1** and **2**, the crystal





Symmetry codes: <sup>i</sup> 2-x, 1-y, 1-z; <sup>ii</sup> 1-x, 1-y, 2-z; <sup>iii</sup> x, 0.5-y, -0.5+z

Fig.3 Arrangement of weak  $\pi$ - $\pi$  stacking interactions in complex **1**

structures including the crystal system and space group are significantly different. The asymmetric unit of complex **2** is shown in Fig.4. Each Pb<sup>II</sup> ion is also chelated by two N atoms from one 2,2'-bipyridine ligand and four O atoms from two 4-methylbenzoate anions (4-MBA). The Pb1-N bond distances are 0.260 8(3) and 0.265 6(3) nm. The Pb1-O bond lengths are in the range of 0.233 3(2) to 0.270 1(2) nm. Among the coordinating bonds around Pb(II), the bond angle (N1-Pb1-O4) is 159.20(9)°. An obvious hole is also observed in the coordination spheres of Pb<sup>II</sup> ions, which indicates the stereochemical activity of the lone pair of electrons (Fig.7). These structure characterizations of the complex **2** are considerably similar to those of complex **1**.

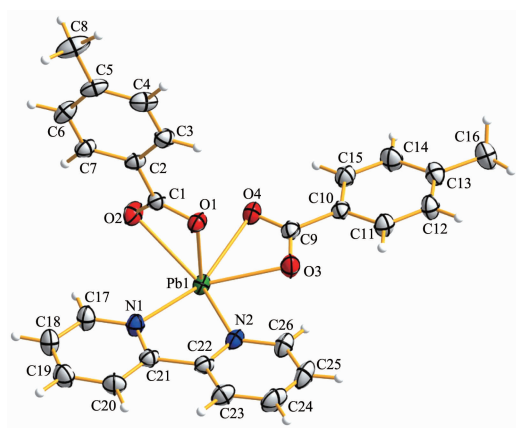
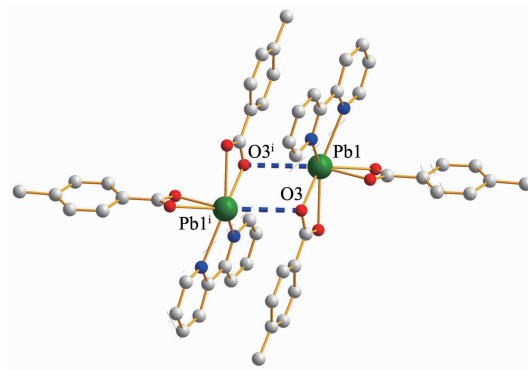


Fig.4 Asymmetric unit of complex **2** with the atom numbering

Different from the complex **1**, the Pb<sup>II</sup> ions adopt the distorted hemidirected environment, which O1 and O2 of carboxylate anion lie in the apical position in complex **2**. The bond angles between Pb1 and the coordinated atoms N1, N2, O3, O4 are 61.75(8)° (N2-Pb1-N1), 77.33(8)° (N2-Pb1-O3), 50.77(8)° (O3-Pb1-O4), and 159.20(9)° (O4-Pb1-N1), respectively. The sum of them is 349.05°, which is close to 360° to some extent. Therefore, the atoms N1, N2, O3, O4 and Pb1 lie in the equatorial position, and the carboxyl oxygen atoms O1 and O2 lie in the apical position of the same side of the equatorial plane.

Another different from the complex **1**, there exist the weak interactions of lead(II) with oxygen atoms of an adjacent molecule, which produce dimer units in the solid state. It is interesting that there is a weak Pb...Pb interactions with a distance of 0.445 84(5) nm by forming a Pb<sub>2</sub>O<sub>2</sub> unit, which can be compared to the reported values<sup>[19-20]</sup>. In fact, each Pb atom in this structure with six normal bonds forms two weak Pb...O bonds, as shown in Fig.5. Only one of them is symmetry independent and the exact distances is Pb1...O3<sup>i</sup> 0.318 5(2) nm, which are in accordance with these reported in the literature (symmetry code: <sup>i</sup> -x, -y, 1-z)<sup>[21-24]</sup>. The presence of a lone pair of electrons on the lead atom is apparently the reason that the bridging interactions are so long. Unlike the literatures have reported<sup>[4,21]</sup>, the secondary Pb...O or Pb...N interactions have lead to the conversion of the hemidirected to holodirected coordination environment around lead(II). In the dimer of complex **2**, the existence of the long additional bonds Pb1...O3<sup>i</sup> (0.318 5(2) nm) hasn't changed the coordina-



Symmetry code: <sup>i</sup> -x, -y, 1-z

Fig.5 Dimer structure of the complex **2**

ting geometries (Fig.7). For example, the bond angle of  $\text{O2-Pb1}\cdots\text{O3}^{\text{i}}$  is  $147.72(7)^\circ$ , which demonstrates there also exists a vacancy in the coordination spheres of  $\text{Pb}^{\text{II}}$  ions and the stereochemistry of the lone pair electrons is active, even though the presence of secondary  $\text{Pb}\cdots\text{O}$  interactions for the complex **2**.

In addition to the weak interaction ( $\text{Pb1}\cdots\text{O3}$ ), there also exist three kinds of weak inter-molecular  $\pi\cdots\pi$  stacking interactions. As shown in Fig.6, the benzene ring ( $\text{C2, C3, C4, C5, C6, C7}$ , centroid  $\text{C}_g^{\text{i}}$ ) and the neighboring ring (centroid  $\text{C}_g^{\text{i}}$ , symmetry code:  $^{\text{i}} 1-x, 1-y, -z$ ) are parallel highly with  $d_{\text{C-C}}=0.430\ 66\ \text{nm}$ ,  $d_{\text{P-P}}=0.339\ 28\ \text{nm}$  and  $\theta=0.379^\circ$ . Similarly, the benzene ring ( $\text{C10, C11, C12, C13, C14, C15}$ , centroid  $\text{C}_g^{\text{ii}}$ ) and the adjacent pyridyl ring ( $\text{N1, C17, C18, C19, C20, C21}$ , centroid  $\text{C}_g^{\text{ii}}$ , symmetry code:  $^{\text{ii}} 2-x, 2-y, 1-z$ ) are also parallel with  $d_{\text{C-C}}=0.389\ 62\ \text{nm}$ ,  $d_{\text{P-P}}=0.357\ 64\ \text{nm}$  and  $\theta=6.213^\circ$ . Moreover, the pyridyl ring (centroid  $\text{C}_g^{\text{iii}}$ ) and the

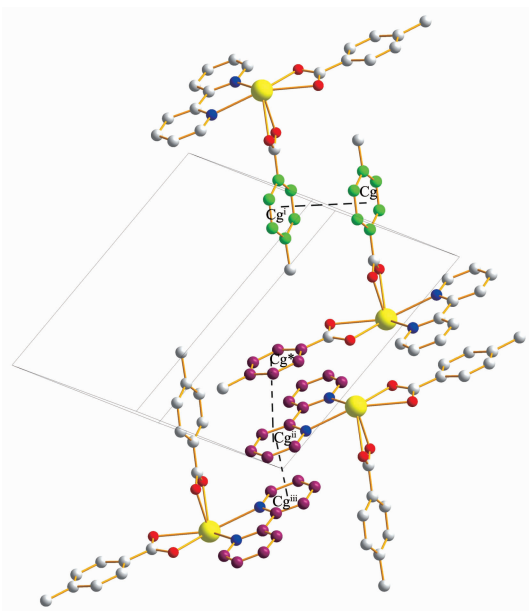
adjacent ring (centroid  $\text{C}_g^{\text{iii}}$ , symmetry code:  $^{\text{iii}} x, y, 1+z$ ) are parallel highly with  $d_{\text{C-C}}=0.360\ 73\ \text{nm}$ ,  $d_{\text{P-P}}=0.344\ 71\ \text{nm}$  and  $\theta=0^\circ$ . The complex **2** are constructed by the secondary ( $\text{Pb}\cdots\text{O}$ ) interactions and weak  $\pi\cdots\pi$  stacks into a stable three-dimensional supramolecular structure.

## 2.2 IR spectral analysis

In the spectra of compounds **1** and **2**, the COOH characteristic peaks near  $1\ 680\ \text{cm}^{-1}$  are absent, indicating that the carboxyl groups in 4-HOBAH and 4-MBAH ligands are deprotonated. In the region where  $\nu(\text{O-H})$  phenoxo deformation occurs, two absorption bands are observed at  $1\ 449$  and  $1\ 426\ \text{cm}^{-1}$  for the complex **1** because the hydroxyl groups of 4-HOBAH all are nonbonding with  $\text{Pb}^{\text{II}}$  ions. In the IR spectra of complex **1**, the  $\nu(\text{O-H})$  stretching frequency of the broad bond around  $3\ 400\ \text{cm}^{-1}$  indicates the presence of free  $\text{H}_2\text{O}$  molecules. The IR spectra of compounds **1** and **2** show typical asymmetric and symmetric carboxylate stretching bonds at  $1\ 547$  and  $1\ 480\ \text{cm}^{-1}$  for **1** and at  $1\ 533$  and  $1\ 458\ \text{cm}^{-1}$  for **2**, respectively. The  $\Delta\nu(\nu_{\text{as}}(\text{COO}^-)-\nu_{\text{s}}(\text{COO}^-))$  for complex **1** and **2** is 67 and  $75\ \text{cm}^{-1}$ , indicating that the carboxylates act as bidentate chelating coordination mode. The vibration bonds at  $1\ 609\sim 1\ 608$ ,  $1\ 008\sim 1\ 007$  and  $781\sim 782\ \text{cm}^{-1}$  could be assigned to the characteristic peaks of 2,2'-bipy molecules. Compared to those of free 2,2'-bipy ( $1\ 585$ ,  $995$  and  $760\ \text{cm}^{-1}$ ), these peaks shift to some extent, indicating that 2,2'-bipy has participated in coordination with  $\text{Pb}^{\text{II}}$  ions in these two complexes. Additionally, the weak bond at  $485$  and  $477\ \text{cm}^{-1}$  may be assigned to the vibrations of  $\text{Pb-O}^{[25]}$  bond for the complex **1** and **2**, respectively. The above analyses are consistent with the crystal structure.

## 2.3 UV absorption and PL spectra

The electronic absorption spectra of the free ligands and the complex **1** and **2** were recorded in DMSO solvent ( $c=0.1\ \text{mmol}\cdot\text{L}^{-1}$ ). UV spectra exhibits the strongest absorption peaks at approximate 281, 270 and 284 nm for the ligand 4-HOBAH, 4-MBAH and 2,2'-bipy, respectively. These absorption are likely due to  $\pi\rightarrow\pi^*$  transition of ligands. Compared to the free ligands, the enhancement and red-shift of the



Symmetry codes:  $^{\text{i}} 1-x, 1-y, -z$ ;  $^{\text{ii}} 2-x, 2-y, 1-z$ ;  $^{\text{iii}} x, y, 1+z$

Fig.6 Arrangement of weak  $\pi$ - $\pi$  stacking interactions in complex **2**

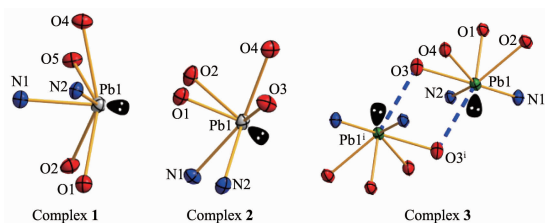


Fig.7 Coordination environment of Pb atoms in complex **1** and **2**, showing secondary  $\text{Pb}\cdots\text{O}$  interaction

absorption bands of complex **1** and **2** (**1**: 290 nm; **2**: 278 nm) probably attribute to the chelating of the ligands to  $\text{Pb}^{\text{II}}$  ion which effectively increase the conjugated extent of the complexes.

The solid-state photoluminescent spectra of compounds **1** and **2** at room temperature upon excitation 319 and 316 nm have been measured. The excitation spectra were recorded in the range of 200~360 nm, setting 458 nm as the emission wavelength, in which there are broad peaks between 290~340 nm (Fig.8). The weak emission occurs at 406 nm for **1** and 405 nm for **2**, corresponding to the  $S_0 \rightarrow S_1$  ( $\pi \rightarrow \pi^*$ ) absorption. Moreover, there are maximum emission peaks at 458 nm in these two complexes, which are red-shifted about 20 and 22 nm compared to that of free ligand (4-HOBAH: 438 nm and 4-MBAH: 436 nm). Obviously, this strong emission come from the aromatic carboxylate ligand, and the large red-shift effect may be attributed to the coordination or an excited state of a metal-perturbing intraligand.

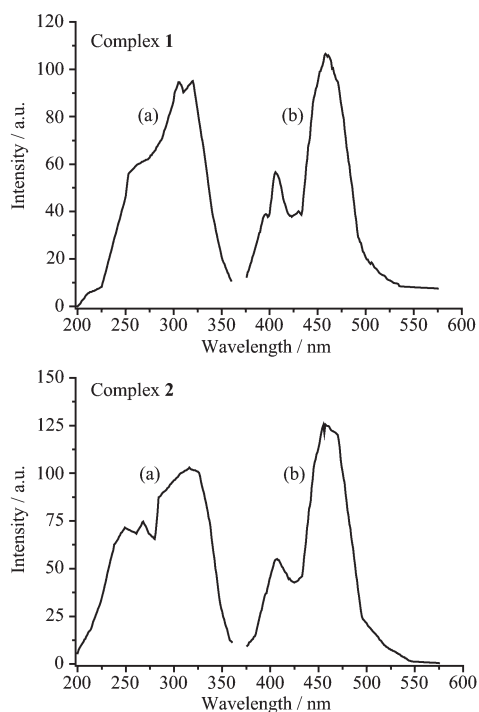


Fig.8 Excitation (a) and emission (b) spectra for the complex **1** and **2**

## 2.4 Thermal properties

Thermal stability studies were performed for complex **1** and **2** in 30~700 °C under  $\text{N}_2$  stream. The

thermal decomposition process of complex **1** can be divided into three stages. The initial weight loss occurs in the range of 30 to 152 °C, corresponding to an endothermic peak, and the TG curve shows that the weight loss corresponding to this temperature range is 2.66% that roughly coincides with the theoretical value of 2.75%, calculated for the loss of one free water molecule. On further heating, two exothermic peaks successively at 346 and 487 °C in the DSC curve and a continued weight loss occurs in the TG curve. Then, a strong exothermic peak at 532 °C accompanied with further decomposition of the compound, and the final solid product is likely to  $\text{PbO}$  when the temperature is above 565 °C.

Thermogravimetric analysis of complex **2** revealed that it is thermally stable up to 300 °C. Above this temperature, a two-step weight loss was observed until 570 °C. The total weight loss of 65.84% is in accordance with the loss of one 2,2'-bipy ligand and two 4-MBAH ligands (calcd. 64.78%). The remaining weight of 34.16% corresponds to the percentage (35.22%) of the Pb and O components, indicating about the final product is also  $\text{PbO}$ .

## References:

- [1] LIU Da-Jun (刘大军), HE Xing-Quan (何兴权), GAO Zheng-Guo (高正国), et al. *Acta Chim. Sinica*(*Huaxue Xuebao*), **2008**,**66**(5):563-566
- [2] Alvarado R J, Rosenberg J M, Andreu A, et al. *Inorg. Chem.*, **2005**,**44**:7951-7959
- [3] Fan S R, Zhu L G. *Inorg. Chem.*, **2006**,**45**:7935-7942
- [4] Shimoni-Livny L, Glusker J P, Bock C W. *Inorg. Chem.*, **1998**, **37**:1853-1867
- [5] Power P P. *Chem. Rev.*, **1999**,**99**:3463-3504
- [6] LI Wei(李 薇), LI Yong-Hong(李昶红), YANG Ying-Qun(杨颖群), et al. *Chinese J. Inorg. Chem.*(*Wuji Huaxue Xuebao*), **2008**,**24**(7):1051-1055
- [7] ZHUO Xin(卓 馨), WEI Xian-Wen(魏先文), GUO Cui-Lian(郭翠莲), et al. *Chinese J. Inorg. Chem.*(*Wuji Huaxue Xuebao*), **2007**,**23**:1029-1034
- [8] TAN An-Zhi(谭安治), WEI You-Huan(韦友欢), CHEN Zi-Lu(陈自卢), et al. *Chinese J. Inorg. Chem.*(*Wuji Huaxue Xuebao*), **2006**,**22**(3):394-398
- [9] Li J T, Yang J. *Acta Cryst.*, **2009**,**E65**:m989



- [10]FU Feng(付 锋), CHEN San-Ping(陈三平), REN Yi-Xia(任宜霞), et al. *Acta Chim. Sinica(Huaxue Xuebao)*, **2008**,**66**(14):1663-1668
- [11]Claudio E S, Goodwin H A, Magyar J S. *Prog. Inorg. Chem.*, **2003**,**51**:1-144
- [12]Hancock R D, Reibenspies J H, Maumela H. *Inorg. Chem.*, **2004**,**43**:2981-2987
- [13]Vicente M, Bastida R, Lodeiro C, et al. *Inorg. Chem.*, **2003**,**42**:6768-6779
- [14]Sheldrick G M. *SADABS*, University of Göttingen, Germany, **1996**.
- [15]Sheldrick G M. *SHELX-97, Program for the Solution and the Refinement of Crystal Structures*, University of Göttingen, Germany, **1997**.
- [16]Shi Y J, Li L H, Li Y Z, et al. *Polyhedron*, **2003**,**22**:917-923
- [17]Soudi A A, Marandi F, Morsali A, et al. *Inorg. Chem. Commun.*, **2005**,**8**:773-776
- [18]Malandrino G, Nigro R L, Rossi P, et al. *Inorg. Chim. Acta*, **2004**,**357**:3927-3933
- [19]Xiao H P, Morsali A. *Helv. Chim. Acta*, **2005**,**88**:2543-2548
- [20]Morsali A, Mahjoub A R. *Helv. Chim. Acta*, **2004**,**87**:2717-2722
- [21]Yuan Y Z, Zhou J, Liu X, et al. *Inorg. Chem. Commun.*, **2007**,**10**:475-478
- [22]Morsali A, Mahjoub A. *Inorg. Chem. Commun.*, **2004**,**7**:915-918
- [23]Mahjoub A R, Morsali A. *Polyhedron*, **2002**,**21**:1223-1227
- [24]Wang L Y, Wang Y F, Ma L F. *Inorg. Chem. Commun.*, **2007**,**10**:1444-1447
- [25]XU Ji-Gui(徐基贵), PAN Zhao-Rui(潘兆瑞), ZHENG He-Gen(郑和根). *Chinese J. Inorg. Chem.(Wuji Huaxue Xuebao)*, **2009**,**25**(9):1551-1556